Supporting Information

Neural and behavioral control in *Caenorhabditis elegans* by a yellow-light-activatable caged compound

Hironori Takahashi[a,c], Mako Kamiya[a,f], Minoru Kawatani[a], Keitaro Umezawa[a], Yoshiaki Ukita[d], Shinsuke Niwa[e], Toshiyuki Oda[c,*], Yasuteru Urano[a,b,g,*]

[a]Graduate School of Medicine and [b]Graduate School of Pharmaceutical Sciences, The University of Tokyo, 7-3-1 Hongo, Bunkyo-ku, Tokyo 113-0033, Japan
[c]Department of Anatomy and Structural Biology, Graduate School of Medicine, University of Yamanashi, 1110 Shimokato, Chuo, Yamanashi 409-3898, Japan
[d]Department of Mechanical Engineering, University of Yamanashi, 4-3-11 Takeda, Kofu 400-8511, Japan
[e]Frontier Research Institute for Interdisciplinary Sciences (FRIS), Tohoku University, Aramaki Aza Aoba 6-3, Aobaku, Sen-dai, Miyagi 980-8578, Japan
[f]PRESTO (Japan) Science and Technology Agency 4-1-8 Honcho, Kawaguchi, Saitama 332-0012, Japan
[g]CREST (Japan) Agency for Medical Research and Development (AMED) 1-7-1 Otemachi, Chiyoda-ku, Tokyo 100-0004, Japan

*Corresponding authors: Toshiyuki Oda, Yasuteru Urano
Email: toda@yamanashi.ac.jp, uranokun@m.u-tokyo.ac.jp

Table of Contents

Supplementary Figures

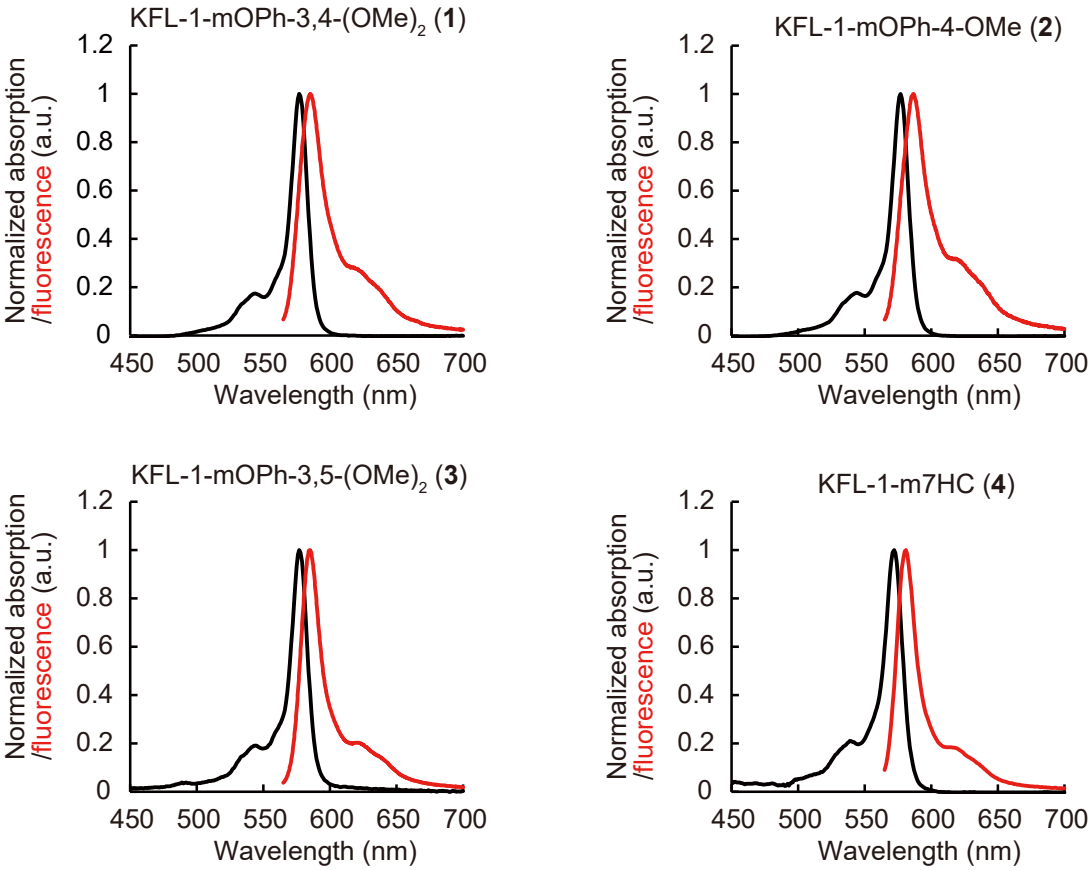

Figure S1. Absorption and fluorescence spectra of aryloxy KFL-1 derivatives.

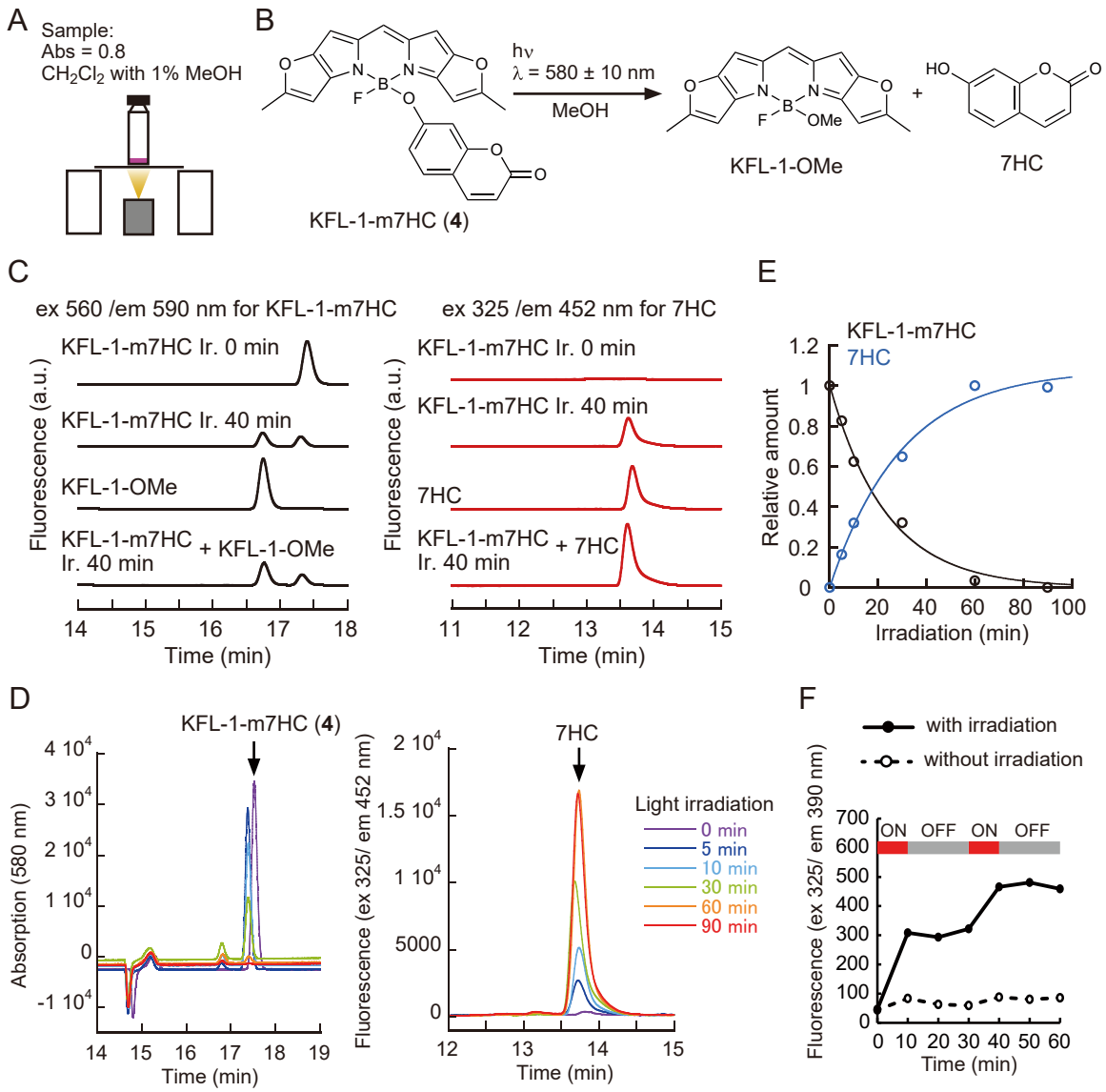

Figure S2. Analysis of the uncaging reaction of KFL-1-m7HC (**4**). (A) Schematic illustration of light irradiation. Aryloxy KFL-1 derivatives were irradiated with 580 ± 10 nm visible light in a cuvette with a bottom area of 1 cm^2. (B) Scheme of the uncaging reaction of KFL-1-m7HC (**4**). (C) HPLC chromatograms of KFL-1-m7HC (**4**) after irradiation. The photoreaction was monitored in terms of the fluorescence of KFL-1-m7HC (**4**) (ex 560/em 590 nm) and 7HC (ex 325/em 452 nm). Before irradiation (Ir. 0 min), the peak of KFL-1-m7HC (**4**) was detected at around 17.3 min, while 7HC was not detected. After 40 min irradiation, two additional peaks were detected at around 16.8 (black line) and 13.6 min (red line). These peaks overlapped with the peaks of the standard samples of KFL-1-OMe (16.8 min) and 7HC (13.6 min), respectively. This indicates that KFL-1-m7HC (**4**) was consumed by the photoreaction and KFL-1-OMe and 7HC were produced. (D) After an appropriate irradiation period (580 ± 10 nm, 26.2 mW cm^{-2}), the solution of KFL-1-m7HC (**4**) was

analyzed using HPLC. KFL-1-m7HC (**4**) was consumed and 7HC was produced in a time-dependent manner. (E) The relative amount of remaining KFL-1-m7HC (**4**) or 7HC was plotted against the irradiation time, normalized by the initial amount of KFL-1-m7HC (**4**) or by the final amount of 7HC, respectively. The time-course was fitted with a single exponential curve. (F) Fluorescence traces of a 1.3 μM solution of KFL-1-m7HC (**4**) with (solid line) or without (dashed line) intermittent light irradiation at 580 ± 10 nm (21.4 mW cm^{-2}). The production of 7HC was monitored with a fluorescence spectrophotometer.

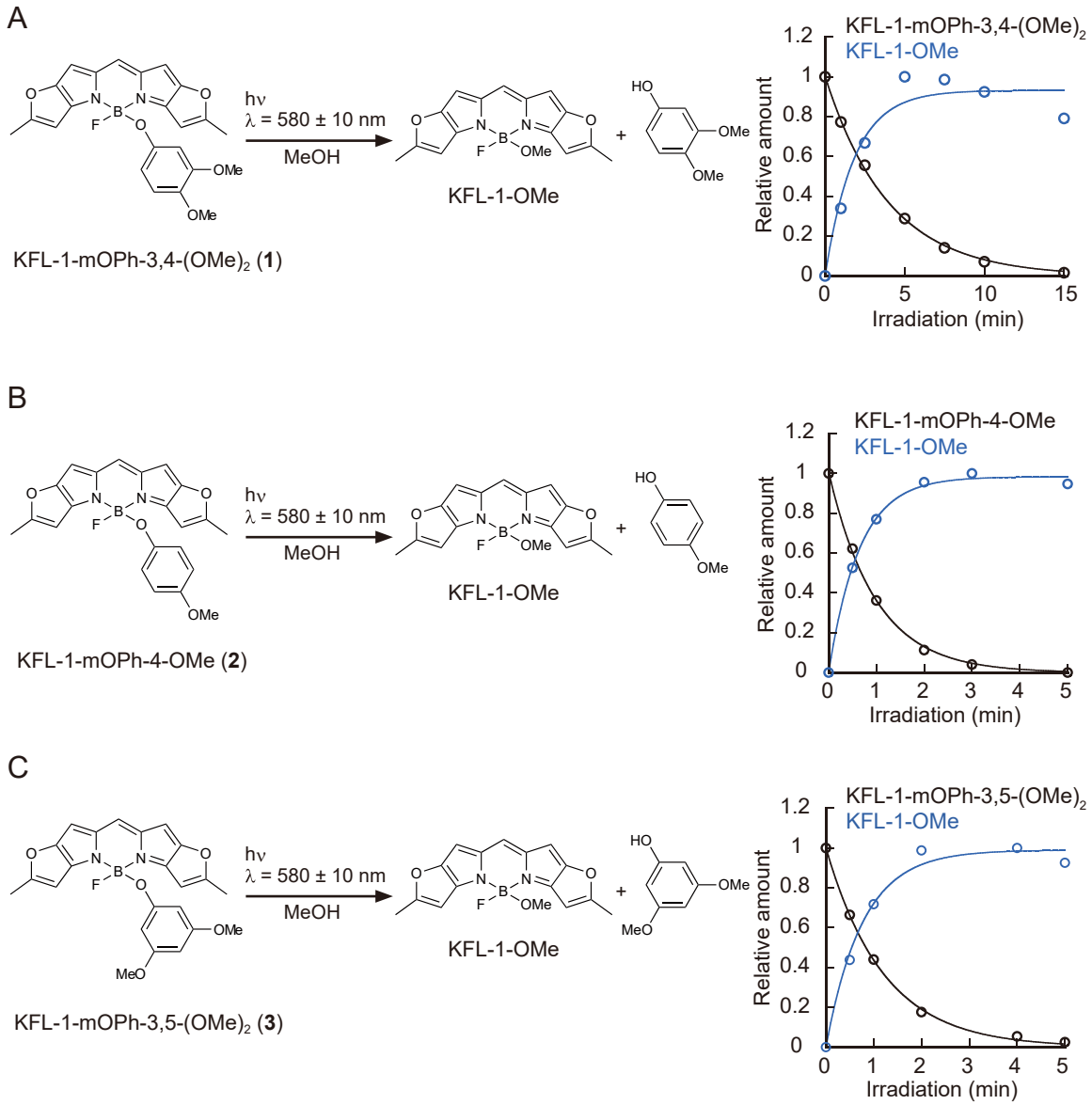

Figure S3. Uncaging reaction of aryloxy KFL-1 derivatives and exponential fitting curves. The black and blue colors in each graph represent the remaining amount of KFL-1 caged compound and the produced amount of KFL-1-OMe, respectively. The amounts of these compounds were normalized by the maximum amount. (A) KFL-1-mOPh-3,4-$(OMe)_2$ (**1**) (580 ± 10 nm, 22.0 mW cm^{-2}). (B) KFL-1-mOPh-4-OMe (**2**) (580 ± 10 nm, 24.5 mW cm^{-2}). (**c**) KFL-1-mOPh-3,5-$(OMe)_2$ (**3**) (580 ± 10 nm, 25.7 mW cm^{-2}).

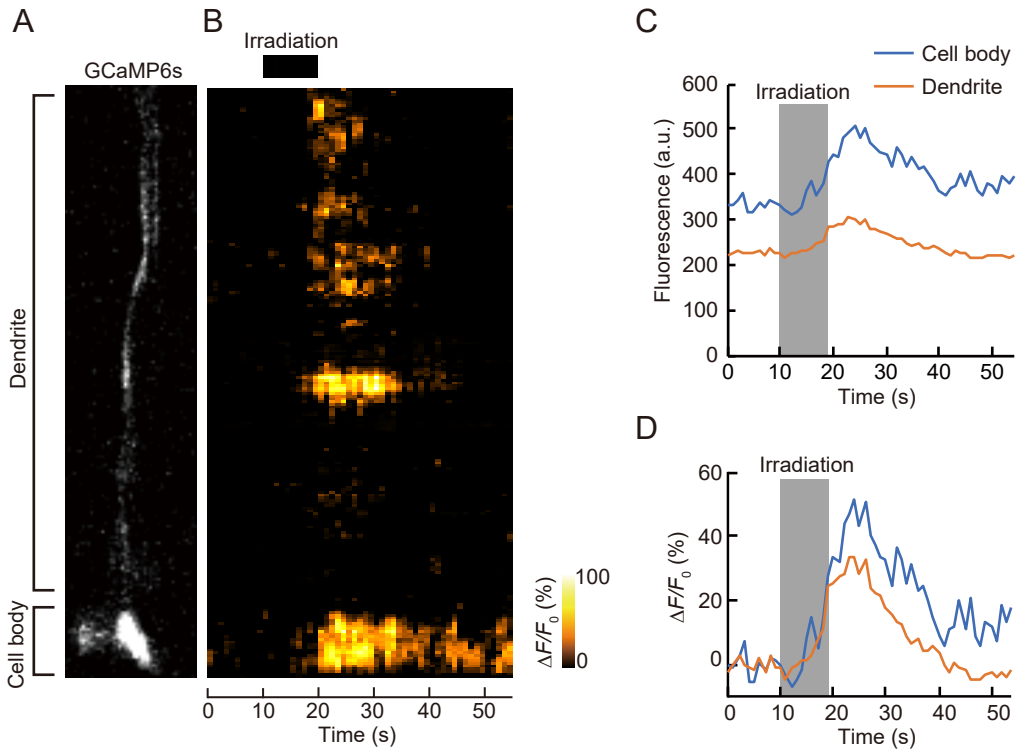

Figure S4. Representative Ca^{2+} response in the cell body and dendrite of an ASH neuron. (A) Fluorescence of GCaMP6s in an ASH neuron captured with a confocal laser scanning microscope. (B) Heatmap displaying the normalized fluorescence change of GCaMP6s ($\Delta F/F_0$) along the cell body and dendrite over time. (C) Representative traces of fluorescence intensity in the cell body and dendrite. (D) Normalized fluorescence change ($\Delta F/F_0$) calculated from data in **c**.

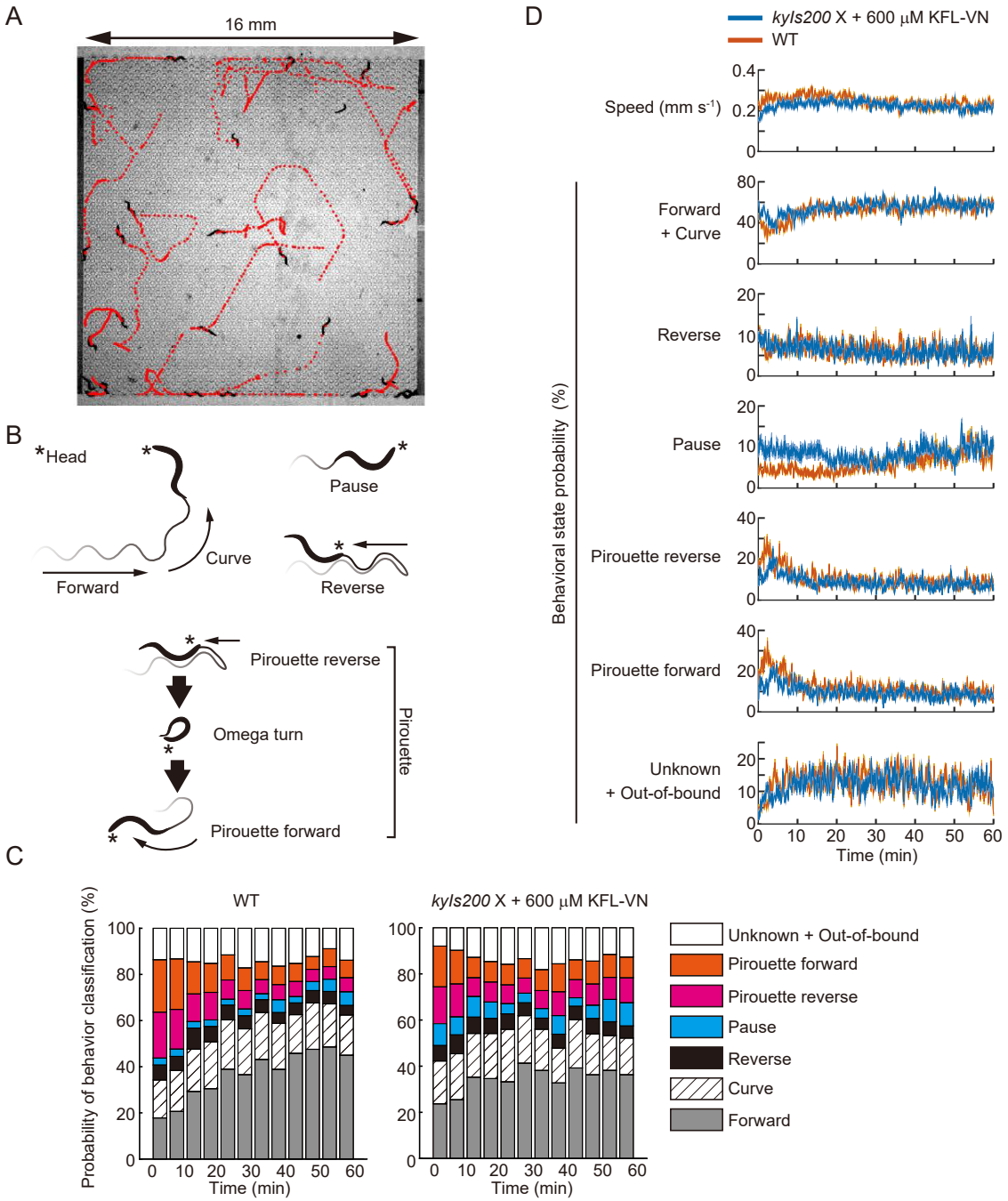

Figure S5. Behavioral analysis in a microfluidic device without irradiation. (A) To analyze the behavior of *C. elegans*, a 16 × 16 mm^2 behavioral arena was prepared using polydimethylsiloxane (PDMS), a biologically inert silicone, as previously reported (1). Continuous centroid paths of individual worms (animal tracks) were obtained by automated tracking software. Animal tracks are shown in red. (B) Animal tracks were segmented to obtain the six primary behavioral states: forward, curve, pause, reverse, pirouette reverse (reversal before an omega turn), and pirouette forward (the curving portion following an omega turn). Asterisks indicate the head position. Arrows indicate the direction of travel. (C) The behavior of worms was observed without yellow light irradiation.

Wild-type worms removed from bacterial food or *kyIs200* X removed from the mixture of 600 μM KFL-VN and bacterial food were introduced into a behavioral arena with continuous buffer flow and their movements were recorded for 60 min. The fraction of forward and curve movements increased over time and non-forward movements (reverse, pause, and pirouette) decreased in the same manner as previously described (1). Representative experiments are shown (26 worms for each). (D) Time courses of forward speed and behavioral state probabilities are shown averaged across all experiments (six experiments for *kyIs200* X, 163 total worms; five experiments for wild type, 139 total worms) and binned in 5-s increments. Shading around the lines indicates SEM (n = 60 frames per time bin for *kyIs200* X; n = 50 frames per time bin for wild type, see **Supplementary Methods** for details). Importantly, the time courses of reverse and pirouette fractions were similar for *kyIs200* X + KFL-VN without illumination and wild-type worms.

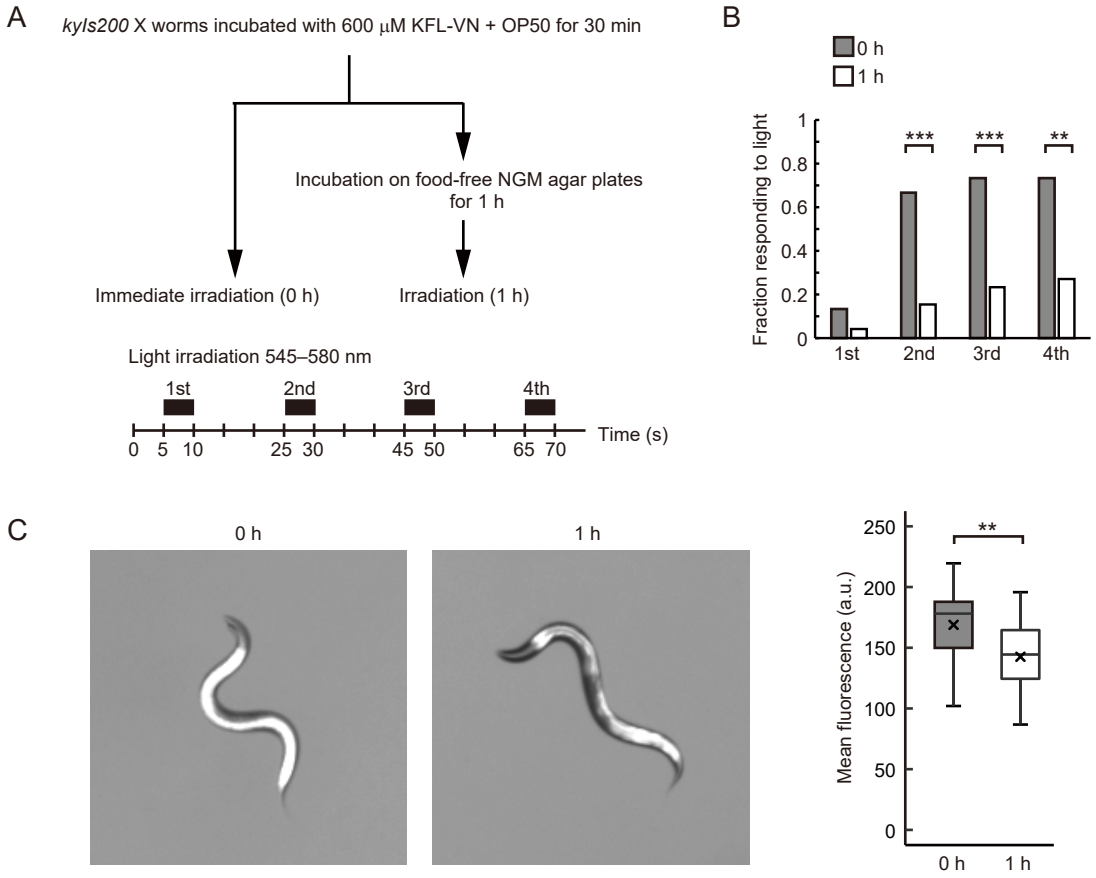

Figure S6. Behavioral assay 1 h after KFL-VN administration. (A) Schema of the experimental procedure. *kyIs200* X worms were incubated on bacteria-KFL-VN (600 μM)-seeded NGM plates for 30 min. The worms were irradiated immediately after feeding or after 1 h incubation on unseeded NGM plates. (B) The fraction of worms showing backward movement during whole-body illumination was plotted (0 h, 0.133 (1st), 0.667 (2nd), 0.733 (3rd), 0.733 (4th); 1 h, 0.038 (1st), 0.154 (2nd), 0.231 (3rd), 0.269 (4th)). n = 30 worms for 0 h, 26 worms for 1 h. $^{**}P < 0.01$, $^{***}P < 0.001$, Fisher's exact test (P = 0.3585 (1st), 0.0001 (2nd), 0.0004 (3rd), 0.0011 (4th)). (C) Fluorescence of KFL-VN during irradiation. Box plots denote mean fluorescence of KFL-VN in worms during first irradiation: line inside the box, median; box edges, interquartile range; whiskers, range without outliers; cross mark, mean. Note that fluorescence of KFL-VN was saturated due to the high concentration of fluorescent KFL-VN and the high-intensity light required for uncaging. Thus, the difference of mean fluorescence between 0 h and 1 h worms does not necessarily reflect the amount of the compound. n = 30 worms for 0 h, 26 worms for 1 h. $^{**}P < 0.01$, Welch's t test (P = 0.0027).

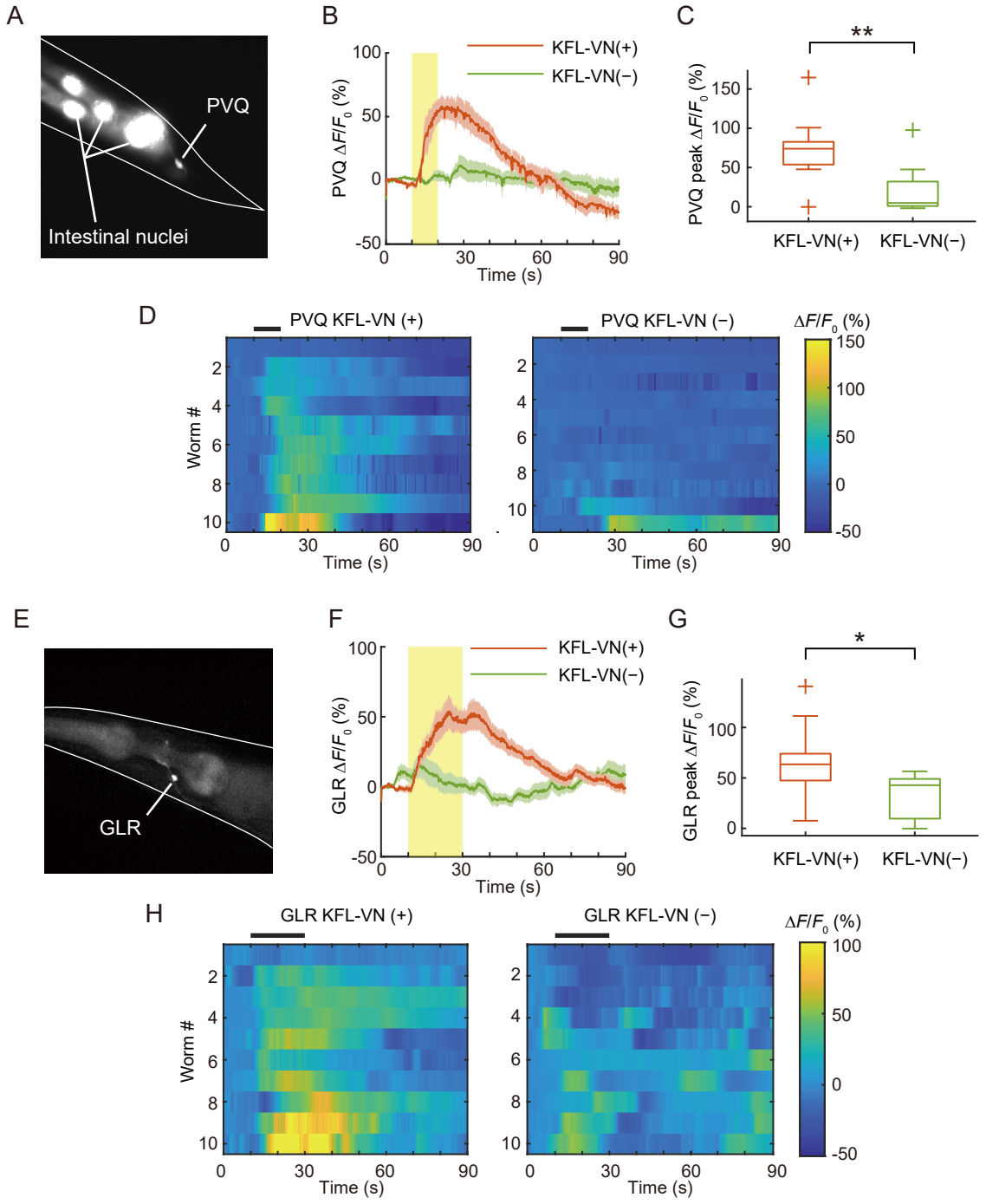

Figure S7. Optical activation of PVQ and GLR. (A) Fluorescence image of GCaMP6s expressed in PVQ neurons under the *sra-6* promoter. As an injection marker, GFP was expressed in intestinal nuclei under the *elt-2* promoter. (B) Averaged PVQ Ca^{2+} responses (onset latency, 2.58 ± 0.45 s). Light stimulation is indicated by a yellow bar. Shaded regions are SEM. (C) Box plots of peak Ca^{2+} responses: line inside the box, median; box edges, interquartile range; whiskers, range without outliers; cross mark, outliers. $^{**}P < 0.01$, Welch's t test ($P = 0.0032$). $n = 10$ worms for KFL-VN (+), 11 worms for KFL-VN (−). (D) Heat maps of PVQ Ca^{2+} responses. Black bars above heat maps

indicate light stimulation (10 s). Ca^{2+} responses are ordered by peak $\Delta F/F_0$. (E) Fluorescence image of GCaMP6s expressed in GLR cells under the *egl-6* promoter. (F) Averaged GLR Ca^{2+} responses. Light stimulation is indicated by a yellow bar. Shaded regions are SEM. (G) Box plots of peak Ca^{2+} responses: line inside the box, median; box edges, interquartile range; whiskers, range without outliers; cross mark, outliers. $*P < 0.05$, Welch's t test ($P = 0.0305$). $n = 10$ worms for KFL-VN (+), 10 worms for KFL-VN (−). (H) Heat maps of GLR Ca^{2+} responses. Black bars above heat maps indicate light stimulation (20 s). Ca^{2+} responses are ordered by peak $\Delta F/F_0$.

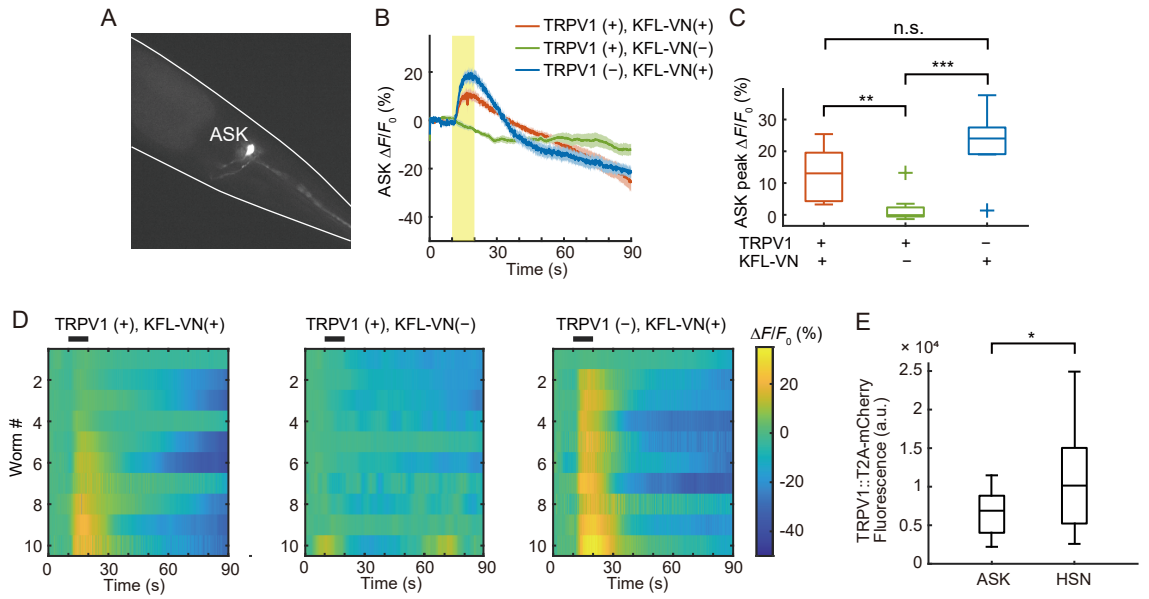

Figure S8. Application of KFL-VN to ASK neurons. (A) Fluorescence image of GCaMP6s expressed in ASK neurons under the *sra-9* promoter. (B) Averaged ASK Ca^{2+} responses. Light stimulation is indicated by a yellow bar. Shaded regions are SEM. (C) Box plots of peak Ca^{2+} responses: line inside the box, median; box edges, interquartile range; whiskers, range without outliers; cross mark, outliers. $^{**}P < 0.01$, $^{***}P < 0.001$, Games-Howell method ($P = 0.0041$ (TRPV1 (+), KFL-VN (+) vs TRPV1 (+), KFL-VN (−)), 0.00007 (TRPV1 (+), KFL-VN (−) vs TRPV1 (−), KFL-VN (+)), 0.0554 (TRPV1 (+), KFL-VN (+) vs TRPV1 (−), KFL-VN (+))). $n = 10$ worms for each experimental condition. (D) Heat maps of ASK Ca^{2+} responses. Black bars above heat maps indicate light stimulation (10 s). Ca^{2+} responses are ordered by peak $\Delta F/F_0$. (E) Comparison of TRPV1 expression between ASK and HSN neurons. Fluorescence of mCherry in the neuronal cell body was measured and plotted as a box plot after subtraction of the local background. Box plot: line inside the box, median; box edges, interquartile range; whiskers, range without outliers. $^{*}P < 0.05$, Welch's t test ($P = 0.0101$). $n = 17$ cells for ASK, 24 cells for HSN.

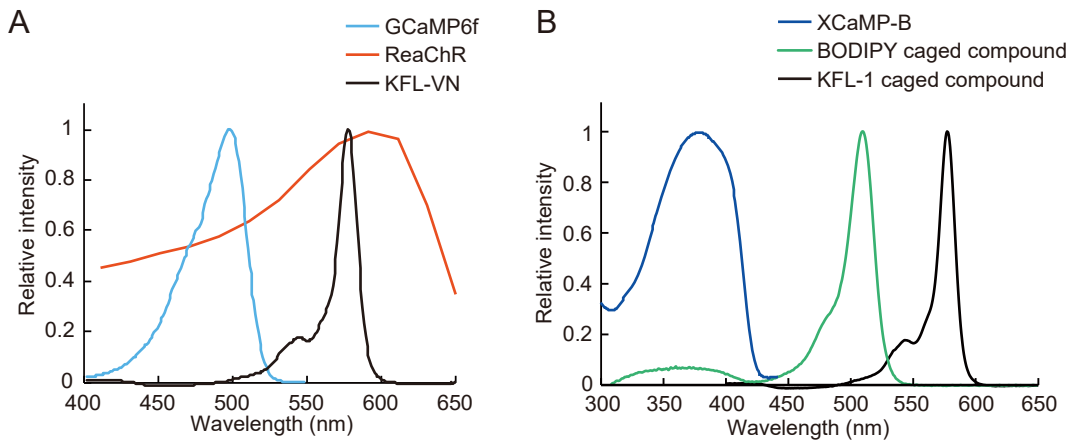

Figure S9. Comparison of absorption or excitation spectra. (A) Absorption spectrum of KFL-VN and excitation spectra of genetically encoded calcium sensor GCaMP6f(2) in the presence of Ca^{2+} (spectral data available at https://www.fpbase.org/) and red-activatable channelrhodopsin (ReaChR) (3). (B) Absorption spectra of BODIPY caged (4) and KFL-1 caged compounds and excitation spectrum of genetically encoded calcium sensor XCaMP-B (5).

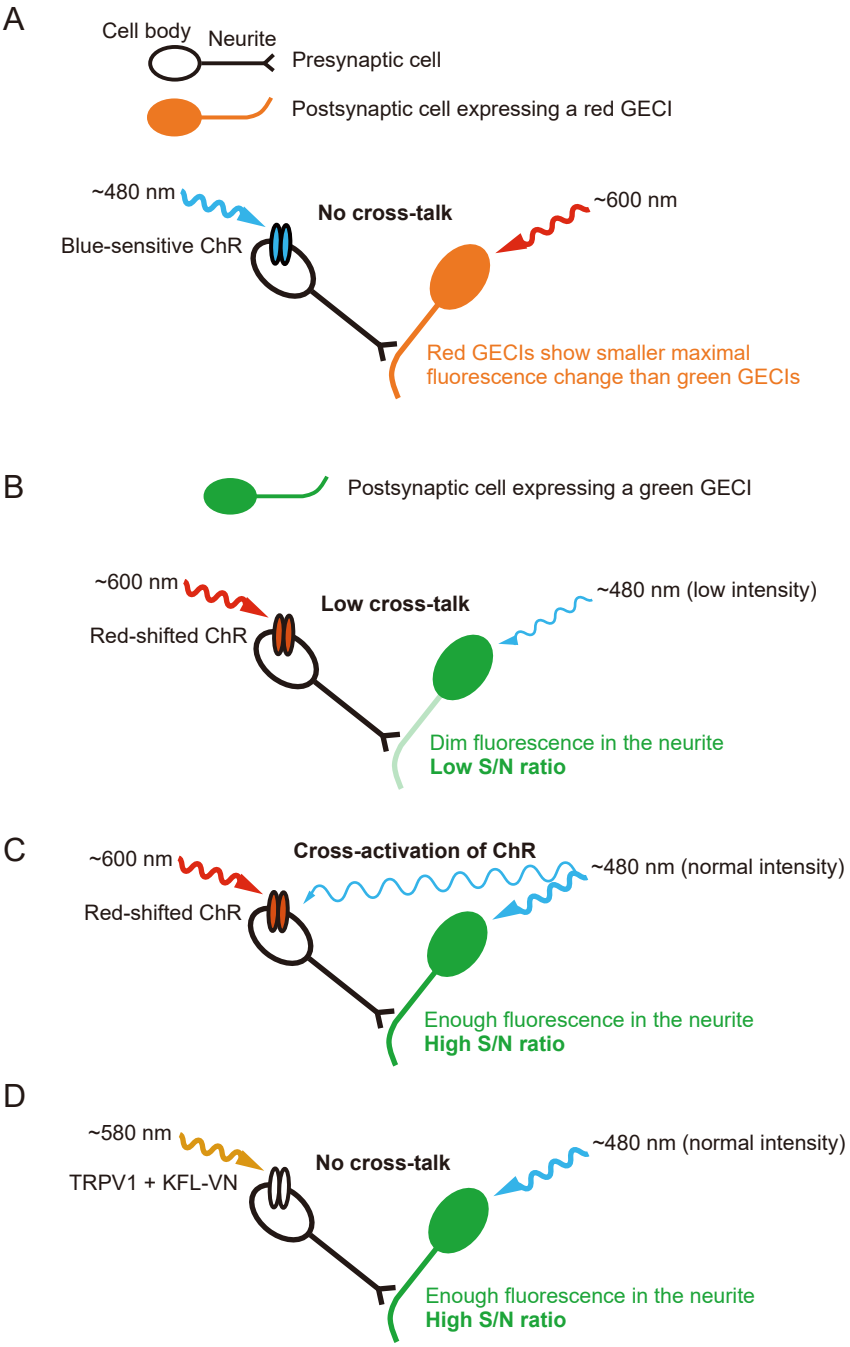

Figure S10. Schematic illustration summarizing simultaneous optical recording and control of neural activity. To optically probe the synaptic connection between two neurons, the activity of the presynaptic cell is manipulated with the light-controlled tool, and the calcium signals of the postsynaptic cell are visualized by means of genetically encoded calcium indicators (GECIs). (A) Simultaneous optical recording and control using blue-sensitive channelrhodopsins (ChRs) and red GECIs. (B) Simultaneous optical recording and control using red-shifted ChRs and green GECIs. Blue light at lower intensity (10% of that normally used) reduces undesired cross-activation of ChRs.

However, calcium responses in the neurite are difficult to detect because of low GECI expression (6). (C) High-intensity blue light (typically 50-100 mW cm^{-2} light is used for observing the fluorescent Ca^{2+} sensor (6, 7)) is required to visualize the neural activity not only in the cell body but also in the neurite, because of lower GECI expression in the neurite. However, blue light at high intensities can activate red-shifted ChRs and induce strong calcium transients in the postsynaptic cell (6). (D) KFL-VN enables simultaneous imaging of the GECI in the neurite without crosstalk between the presynaptic activation and postsynaptic monitoring, because the absorption spectrum of KFL-VN hardly overlaps with that of the GECI (**Figure S9A**)

Supplementary Tables

Table S1. Spectroscopic and photochemical properties of aryloxy KFL-1 derivatives.

Compound	HOMO[a]	λ_{abs} [b] /nm	ε [b]/10^4 /M^{-1} cm^{-1}	λ_{em} [b] /nm	ϕ_{fl} [b]	ϕ_u [b]/10^{-4}	$\varepsilon\phi_u$ [b] / M^{-1} cm^{-1}	τ_c /s	τ_p /s
KFL-1-mOPh-3,4-$(OMe)_2$ (**1**)	-0.200	577	20	585	0.02	1.3	27	239	109
KFL-1-mOPh-4-OMe (**2**)	-0.207	577	20	586	0.03	4.9	98	59	39
KFL-1-mOPh-3,5-$(OMe)_2$ (**3**)	-0.217	577	20	585	0.08	3.7	75	73	46
KFL-1-m7HC (**4**)	-0.233	572	20	581	~1	0.24	4.8	1 401	1 786

[a] HOMO energy level of the corresponding phenol calculated at the B3LYP/6-31G level by Gaussian09 (solvent = dichloromethane). Unit: hartree. [b] Measured in CH_2Cl_2 with 1% MeOH. ϕ_u was calculated using τ_c. λ_{abs}: absorption maximum, ε: molar absorption coefficient, λ_{em}: emission maximum, ϕ_{fl}: fluorescence quantum efficiency, ϕ_u: uncaging quantum efficiency, τ_c: time constant of consumption of KFL-1-caged compounds, τ_p: time constant of production of KFL-1-OMe or 7HC. The ε values of aryloxy KFL-1 derivatives were assumed to be 200,000, according to the literature (8).

Table S2. List of primers used in this study.

Purpose	Forward primer	Reverse primer
sra-6p cloning	TGGGCGCTCGGTGCTCTTACGGTGT	ACGGCGCACATGAAGTCTCAGACTGT
sra-6p insert (InFusion)	acttggaaatgaaatCTGTCATGGTCAGTATTTGAGAAG	agaacccattctagaGGCAAAATCTGAAATAATAAATATTAAATTCTGCG
elt-2p cloning	TTCAAGCTTCATCACGTTACCCGCCCCA	GAGCACACAAGTCCCTGCCGACGGG
elt-2p insert (Gibson Assembly)	taacaacttggaaatgaaatGTTTTTTCAGCTCGACCATTTGGTG	cggaggaggccattctagaTCTATAATCTATTTTCTAGTTTCTATTTTAT
L3558 backbone containing *GCaMP6s* (InFusion)	TCTAGAATGGGTTCTCATCATCATCATCATC	ATTTCATTTCCAAGTTGTTAGCG
L3558 backbone containing *mRFP* (Gibson Assembly)	TCTAGAATGGCCTCCTCCGAGGACGTC	ATTTCATTTCCAAGTTGTTAGCG
egl-6p cloning	TTCAAAATCTGATTCGCTAGCCCACGCTGA	ACGCGTCATCAAAACCACCTCCCGA
egl-6p insert for GCaMP6s	taacaacttggaaatgaaatCCAACATTTCCAGAGAGAACAGAGTCC	gatgagaacccattctagaTGCTGAAAAGCTGTCATTGTGTTCTATG
egl-6p insert for TRPV1	Same as above	agctagcccgttgttccatTGCTGAAAAGCTGTCATTGTGTTCTATG
tdc-1p cloning	GCCTGCCTAGCGCCCGTGTTTTGAA	TGCTTCCTGTCGCTGTCGCCTCACT
tdc-1p insert for GCaMP6s	taacaacttggaaatgaaatGGGAGCAACAGTTATTCTCAAGGGAG	gatgagaacccattctagaTTGGGCGGTCCTGAAAAATGCACCG
tdc-1p insert for TRPV1	Same as above	agctagcccgttgttccatTTGGGCGGTCCTGAAAAATGCACCG
rig-3p cloning	GCGTGCGCGGTTCCCTTTTCTGAGG	CCACCACCCGCGGATTTCGTCGAAA
rig-3p insert for GCaMP6s	taacaacttggaaatgaaatGGAAAAATGTGAGATCTTCGCTGAAA	gatgagaacccattctagaGAATGAAGTTCTTCTGCAAGGAATGAC
rig-3p insert for TRPV1	Same as above	agctagcccgttgttccatGAATGAAGTTCTTCTGCAAGGAATGAC
sra-7p insert for GCaMP6s	taacaacttggaaatgaaatTCAGTCGTTCAACAATAGTGATGCCG	gatgagaacccattctagaGGCTTCTAATATTTCGAGAAACTGCAAAA
sra-9p cloning	TGTTCCCGCGCAAGGATGTACCCATGA	CCAGTTTGCGCAAAAATCATACCGCCTGT

sra-9p insert for GCaMP6s	taacaacttggaaatgaaatGCATGCTATAT TCCACCAAAAGAAAGTT	gatgagaacccattctagaGAAATCTTGAA ACTGAAAAATACAAAAGTG
sra-9p insert for GCaMP6s	Same as above	agctagcccgttgttccatGAAATCTTGAAA CTGAAAAATACAAAAGTG
myo-2p cloning	GCGAGTGAGCCCGCGAGAACA CCAC	TGCCCATGAACATGCGGGCAACG GA
myo-2p insert	CCCAAGCTTCATTTTATATCTGA GTAGTATCCTTTGCTT	CCCTCTAGATTCTGTGTCTGACGA TCGAGGGTTA
Rat *trpv1* cloning	ATGGAACAACGGGCTAGCTTAG ACTCAG	TTATTTCTCCCCTGGGACCATGGA ATCC
trpv1 insert for L3558 (*gfp* replaced by *T2A-mCherry*)	acccacgaccactagatccaATGGAACAA CGGGCTAGCTTAGACTC	gaagagagcctctaccctcTTTCTCCCCTGG GACCATGGAATCC

Small letters indicate overlap sequences required for InFusion or Gibson Assembly system.

Supplementary Movies

Movie S1. Fluorescence change of GCaMP6s induced by uncaging of KFL-VN. ASH neuron was observed with a confocal microscope. Fluorescence images were processed to obtain $\Delta F/F_0$ image stacks using Fiji software (see **Supplementary Methods** for details).

Movie S2. Optical behavior control with KFL-VN in *kyIs200* X strain. After feeding *E. coli* with 535 μM KFL-VN, *kyIs200* X worms were illuminated (545-580 nm light) with a fluorescence stereomicroscope (see **Supplementary Methods** for details). The frame rate for animation is 30 frames s^{-1}, though recording was done at 10 frames s^{-1} (i.e. 3x playback).

Movie S3. No response to KFL-VN uncaging in wild-type strain. Wild-type worms were illuminated after feeding on *E. coli* with 535 μM KFL-VN (3x playback).

Movie S4. Application of KFL-VN to body wall muscles. After feeding *E. coli* with 500 μM KFL-VN, worms expressing GCaMP6s and TRPV1 in body wall muscles were illuminated (560-600 nm light). The frame rate for animation is 30 frames s^{-1}, though recording was done at 10 frames s^{-1} (i.e. 3x playback).

Movie S5. Application of KFL-VN to HSN neurons. After feeding *E. coli* with 1 mM KFL-VN, worms expressing GCaMP6s and TRPV1 in HSN neurons were illuminated (560-600 nm light). The frame rate for animation is 30 frames s^{-1}, though recording was done at 10 frames s^{-1} (i.e. 3x playback).

Supplementary Note

Protein expression in multiple cells via the *sra-6* or *rig-3* promoter

The *sra-6* promoter (*sra-6p*) drives GCaMP6s expression strongly in ASH and PVQ neurons and weakly in ASI neurons (9, 10) (**Figure 3A**). TRPV1-expressing strain *kyIs200* X was created using *sra-6p* (11). Thus, worms used in this study express both TRPV1 and GCaMP6s in these three neuron types. ASI sensory neurons form a reciprocal inhibitory circuit between ASH sensory neurons to modulate worm behaviors (12). In this study, however, ASI neurons seemed not to be activated by uncaging of KFL-VN (data not shown) probably due to the weak expression of TRPV1 and inhibition by activated ASH neurons (12). On the other hand, it is possible that PVQ interneurons might be activated by uncaging of KFL-VN, because they strongly express TRPV1 and GCaMP6s. In behavioral assays (**Figure 4**), whole-body illumination could activate PVQ neurons as shown in **Figure S7 A-D**. The behavioral output was mainly due to ASH activation, because PVQ interneurons do not have a major role in the control of locomotion (10). However, a previous optogenetic study indicated that concomitant activation of multiple cells can affect behavioral output. For example, worms expressing channelrhodopsin in ASH with other neurons showed low response rates to light stimulation (13). In this study, the first light stimulation of *kyIs200* X failed to evoke behavioral responses (**Figure 4B**). It is possible that this failure resulted from TRPV1 expression in multiple cells (ASH, ASI, and PVQ), as described previously (13).

The results of behavioral tests in RIM or AVA interneurons shown in **Figure 6I** also support the above discussion. The *tdc-1* promoter drove expression of GCaMP6s and TRPV1 mainly in RIM with faint or inconsistent expression in RIC (**Figure 6A**) (14), while the *rig-3* promoter led to expression in multiple neurons (AVA, I1, I4, M4, NSM, **Figure 6E**) (15). The behavioral results reflected this expression pattern, in accordance with a previous report (13): 65% of the *tdc-1p* worms and 35 % of the *rig-3p* worms showed reversal responses to light stimulation (**Figure 6I**).

Generally, a single neuron-specific promoter is not always available in *C. elegans* (for example, no ASH-specific promoter has been identified). If specific neuronal activation is needed, it is possible to use the site-specific recombinase Cre or FLP to drive specific expression (12, 16, 17).

The lifetime of the TRPV1 agonist released from KFL-VN

If the TRPV1 agonist released from KFL-VN remains in situ for a long time, it would be problematic. However, because the agonist is a small molecule, it is expected to diffuse away quickly. Indeed, **Figures 3, 5, 6** and **Fig. S7** show that the light-evoked calcium signal returns to baseline after ~20-30 s; this means that the local concentration of the released agonist decreases rapidly when the uncaging light is switched off. Optogenetic studies using GCaMP and Chrimson, a red-shifted channelrhodopsin, in *C. elegans* showed that the light-evoked signal returned to baseline after ~10 s (18, 19). In those studies, GCaMP2 or GCaMP3 was used to monitor the calcium signal, whereas

GCaMP6s was used in this study. The half decay time after 10 action potentials is ~480 ms for GCaMP2 (20), ~610 ms for GCaMP3 (21), and ~1,800 ms for GCaMP6s (2). Thus, the fluorescence signal of GCaMP6s used in this study returns to baseline 3 times more slowly than that of GCaMP2 or GCaMP3. For example, when used for monitoring odor responses in AWA, GCaMP2.2b required ~10 s to return to baseline after odor removal, whereas GCaMP6s required ~20-30 s (6). Overall, the results confirm that the released agonist diffuses away rapidly.

Supplementary Methods

Materials and general instruments

General chemicals were of the best grade available, supplied by Tokyo Chemical Industries, Wako Pure Chemical, or Aldrich Chemical Co. and were used without further purification. Purification by gel permeation chromatography (GPC) was carried out on a Japan Analytical Industry Recycling Preparative HPLC LC-9210 NEXT with a JAIGEL HR column. ^{1}H NMR and ^{13}C NMR spectra were recorded on a Bruker AVANCE III 400 Nanobay at 400 MHz for ^{1}H NMR and 101 MHz for ^{13}C NMR. High-resolution mass spectra (HRMS) were measured with a MicrOTOF (Bruker) with electron spray ionization (ESI).

Chemical synthesis

Keio Fluors-1 (KFL-1) was synthesized as previously reported (8).

Preparation of KFL-1-mOPh-3,4-(OMe)$_2$ (1)

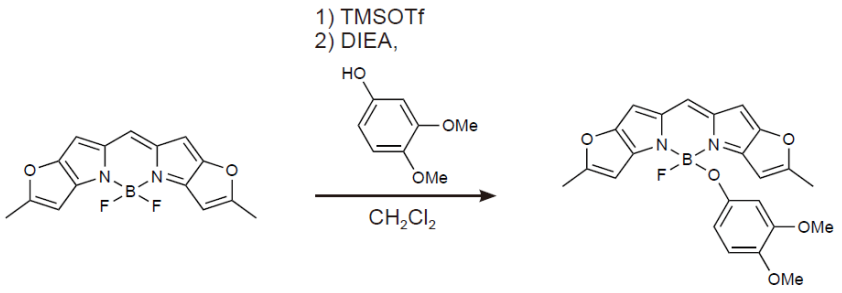

To KFL-1 (10.5 mg, 0.035 mmol, 1 eq.) in dichloromethane (2 ml) was added TMSOTf (32 μl, 0.17 mmol, 5 eq.) in dichloromethane at 4 °C. This solution was kept at 4 °C for 3 minutes, then a solution of 3,4-dimethoxyphenol (53.9 mg, 0.35 mmol, 10 eq.) and DIEA (61 μl, 0.35 mmol, 10 eq.) in dichloromethane (2 ml) was added to it. The reaction mixture was stirred at room temperature for 15 minutes, then poured into water and extracted with dichloromethane. The organic solution was washed with brine, dried over Na_2SO_4, and concentrated in vacuo. The residue was purified by means of column chromatography (silica, eluent: ethyl acetate/hexane = 34/66, v/v) and GPC (with chloroform as an eluent) to yield **1** (2.8 mg, 15.8%) as a dark violet solid. ^{1}H NMR (400 MHz, $CDCl_3$): δ 7.09 (s, 1H), 6.50 (d, J = 8.7 Hz, 1H), 6.40 (s, 2H), 6.26 (d, J = 2.7 Hz, 1H), 6.20 (s, 2H), 6.07 (dd, J = 8.7, 2.7 Hz, 1H), 3.71 (s, 3H), 3.62 (s, 3H), 2.42 (s, 6H); ^{13}C NMR* (101 MHz, $CDCl_3$): δ 169.8, 152.9, 151.0, 149.1, 142.7, 138.2, 127.9, 111.8, 109.4, 104.0, 102.6, 98.3, 56.3, 55.6, 16.0; HRMS (ESI$^+$) *m/z* calcd. for $C_{23}H_{20}BFN_2NaO_5$ $[M+Na]^+$, 457.1346; found, 457.1349 (+0.3 mmu). *One quaternary carbon was not registered due to carbon-fluorine coupling (^{13}C-^{19}F coupling).

Preparation of KFL-1-mOPh-4-OMe (2)

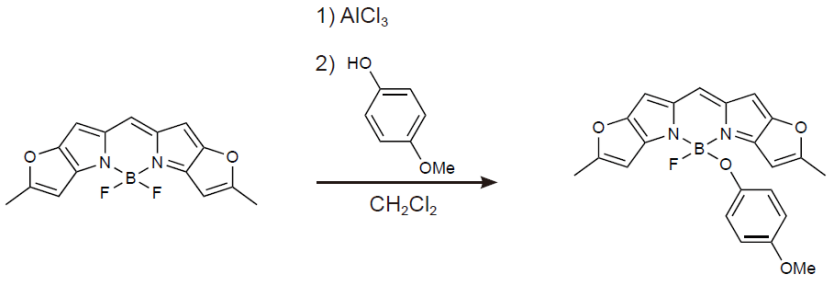

A solution of KFL-1 (19.7 mg, 0.066 mmol, 1 eq.) and $AlCl_3$ (10.5 mg, 0.079 mmol, 1.2 eq.) in dichloromethane (2 ml) was refluxed at 40 °C for 15 minutes. To this solution was added dropwise 4-methoxyphenol (9.8 mg, 0.079 mmol, 1.2 eq.) in dichloromethane (1 ml). The reaction mixture was refluxed for 10 minutes, then poured into sat. $NaHCO_3$ aq., and extracted with dichloromethane. The organic solution was washed with brine, dried over Na_2SO_4, and concentrated in vacuo. The residue was purified by means of column chromatography (silica, eluent: dichloromethane/ethyl acetate = 100/0 to 95/5, v/v) and GPC (chloroform was used as an eluent) to yield **2** (1.6 mg, 6.0%) as a dark violet solid. ^{1}H NMR (400 MHz, $CDCl_3$): δ 7.08 (s, 1H), 6.57 (d, J = 9.2 Hz, 2H), 6.52 (d, J = 9.2 Hz, 2H), 6.39 (s, 2H), 6.19 (s, 2H), 3.65 (s, 3H), 2.41 (s, 6H); ^{13}C NMR* (101 MHz, $CDCl_3$): δ 169.7, 153.3, 152.8, 151.0, 138.2, 128.0, 119.7, 114.3, 102.6, 98.3, 55.6, 16.0; HRMS (ESI$^+$) *m/z* calcd. for $C_{22}H_{18}BFN_2NaO_4$ $[M+Na]^+$, 427.1240; found, 427.1225 (-1.5 mmu). *One quaternary carbon was not registered due to carbon-fluorine coupling (^{13}C-^{19}F coupling).

Preparation of KFL-1-mOPh-3,5-(OMe)$_2$ (3)

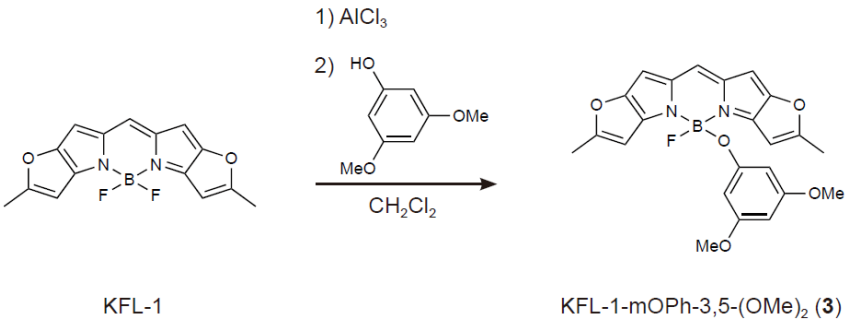

A solution of KFL-1 (6.6 mg, 0.022 mmol, 1 eq.) and $AlCl_3$ (4.4 mg, 0.033 mmol, 1.5 eq.) in dichloromethane (0.5 ml) was refluxed at 40 °C for 10 minutes. To this solution was added dropwise a solution of 3,5-dimethoxyphenol (5.1 mg, 0.033 mmol, 1.5 eq.) in dichloromethane (0.5 ml). The reaction mixture was refluxed for 10 minutes, then poured into sat. $NaHCO_3$ aq., and extracted with dichloromethane. The organic solution was washed with brine, dried over Na_2SO_4, and concentrated

in vacuo. The residue was purified by means of column chromatography (silica, eluent: dichloromethane) and GPC (chloroform was used as an eluent) to yield **3** (trace) as a dark violet solid. ^{1}H NMR (400 MHz, $CDCl_3$): δ 7.14 (s, 1H), 6.42 (s, 2H) ,6.21 (s, 2H), 5.90 (t, J = 2.2 Hz, 1H), 5.82 (d, J = 2.2 Hz, 2H), 3.57 (s, 6H), 2.41 (s, 6H); ^{13}C NMR was not measured because insufficient material was available; HRMS (ESI^+) *m/z* calcd. for $C_{23}H_{20}BFN_2NaO_5$ $[M+Na]^+$, 457.1346; found, 457.1337 (-1.0 mmu).

Preparation of KFL-1-m7HC (4)

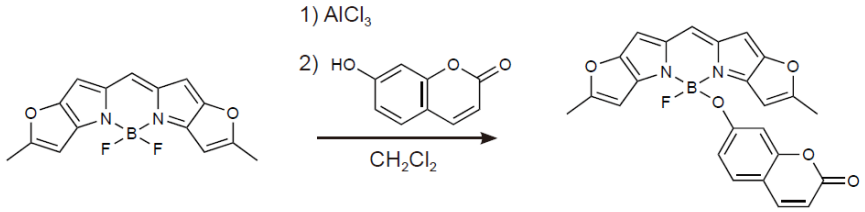

KFL-1 KFL-1-m7HC (**4**)

A solution of KFL-1 (9.9 mg, 0.033 mmol, 1 eq.) and $AlCl_3$ (5.3 mg, 0.040 mmol, 1.2 eq.) in dichloromethane (0.5 ml) was refluxed at 40 °C for 10 minutes. To this solution was added dropwise 7-hydroxycoumarin (6.4 mg, 0.040 mmol, 1.2 eq.) in dichloromethane (0.5 ml). The reaction mixture was refluxed for 10 minutes, then poured into sat. $NaHCO_3$ aq., and extracted with dichloromethane. The organic solution was washed with brine, dried over Na_2SO_4, and concentrated in vacuo. The residue was purified by means of column chromatography (silica, eluent: ethyl acetate/hexane = 34/66, v/v) and GPC (chloroform was used as an eluent) to yield **4** (1.7 mg, 11.7%) as a dark violet solid. ^{1}H NMR (400 MHz, $CDCl_3$): δ 7.50 (d, J = 9.4Hz, 1H), 7.20 (s, 1H), 7.15 (d, J = 8.6 Hz, 1H), 6.70 (dd, J = 8.6, 2.3 Hz, 1H),6.47 (s, 2H), 6.36 (d, J = 2.2 Hz, 1H), 6.18 (s, 2H), 6.10 (d, J = 9.4 Hz, 1H), 2.41 (s, 6H); ^{13}C NMR (101 MHz, $CDCl_3$): δ 170.3, 161.9, 160.8, 155.8, 152.9, 150.8, 143.8, 138.2, 128.5, 128.2, 116.7, 112.3, 112.1, 105.3, 103.4, 97.9, 16.1; HRMS (ESI^+) *m/z* calcd. for $C_{24}H_{16}BFN_2NaO_5$ $[M+Na]^+$, 465.1033; found, 465.1027 (-0.6 mmu).

Preparation of KFL-VN (5)

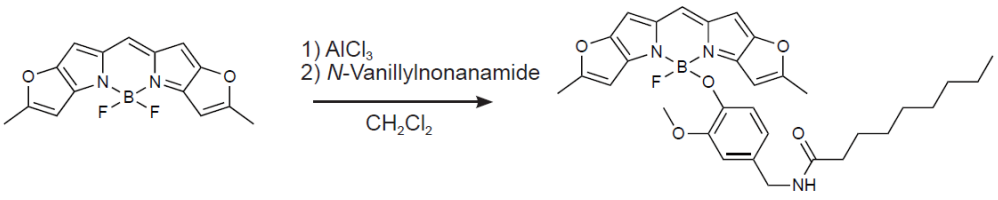

KFL-1 KFL-VN (**5**)

A solution of KFL-1 (35.3 mg, 0.12 mmol, 1 eq.) and $AlCl_3$ (23.5 mg, 0.18 mmol, 1.5 eq.) in dichloromethane (1 ml) was refluxed at 40 °C for 10 minutes. To this solution was added dropwise

N-vanillylnonanamide (345.2 mg, 1.18 mmol, 10 eq.) in dichloromethane (1 ml). The reaction mixture was refluxed for 15 minutes, then poured into water and extracted with dichloromethane. The organic solution was washed with brine, dried over Na_2SO_4, and concentrated in vacuo. The residue was purified by means of column chromatography (silica, eluent: ethyl acetate/hexane = 50/50, v/v) and GPC (chloroform was used as an eluent) to yield **5** (6.1 mg, 9.0%) as a dark violet solid. ^{1}H NMR (400 MHz, $CDCl_3$): δ 7.09 (s, 1H), 6.64 (d, *J* = 2.0 Hz, 1H), 6.42 (dd, *J* = 8.1, 2.1 Hz, 1H), 6.38 (s, 2H), 6.24 (d, *J* = 8.1 Hz, 1H), 6.21 (s, 2H), 5.53 (s, 1H), 4.23 (d, *J* = 5.52 Hz, 2H), 3.75 (s, 3H), 2.40 (s, 6H), 2.13 (t, *J* = 7.4 Hz, 2H), 1.63-1.57 (m, 2H), 1.25-1.24 (m, 10H), 0.87 (t, *J* = 6.9 Hz, 3H); ^{13}C NMR* (101 MHz, $CDCl_3$): δ 172.9, 169.5, 151.1, 145.7, 138.2, 130.0, 127.9, 120.0, 118.1, 111.5, 102.6, 98.4, 55.7, 43.7, 37.0, 31.9, 29.5, 29.4, 29.3, 25.9, 22.8, 16.0 14.2; HRMS (ESI^+) *m/z* calcd. for $C_{32}H_{37}BFN_3NaO_5$ $[M+Na]^+$, 596.2708; found, 596.2682 (-2.6 mmu). *Some carbon peaks disappeared due to carbon-fluorine coupling (^{13}C-^{19}F coupling).

Spectroscopic measurements

The optical properties of KFL-1 derivatives were examined using a UV-2450 UV-VIS spectrophotometer (Shimadzu) and an F-7000 fluorescence spectrophotometer (Hitachi). Quantum efficiencies of fluorescence (ϕ_{fl}) were measured with a Quantaurus-QY C11347-12 (Hamamatsu Photonics).

Quantification of photoreaction of KFL-1 derivatives

The quantum yields of single-photon photolysis (ϕ_u) were determined by exponential fitting of substrate consumption. Solutions (100 μl) of aryloxy KFL-1 derivatives in dichloromethane containing 1% methanol (Abs = 0.8) were irradiated with 580 ± 10 nm visible light from a Xe lamp (MAX303, Asahi Bunko) equipped with a band-pass filter MX0580 (Asahi Bunko). After an appropriate irradiation period, 4 μl of the solution was removed for analysis by reversed-phase HPLC. The analysis was carried out on an Inertsil ODS-3 (4.6 × 250 mm) column using an HPLC system composed of a pump (Jasco, PU-2080 or PU-2087) and a detector (Jasco, MD-2010). As eluents, 0.1 M triethylamine-acetate buffer, H_2O, acetonitrile and methanol were used. The increase of the product and decrease of the KFL-1 derivative were quantified based on the peak area in the fluorescence or absorption chromatogram. The time constant τ was determined by fitting the resulting time-course of the amount of substrate or product with a single exponential curve. Uncaging quantum efficiency ϕ_u was calculated according to the following equation.

$$\phi_u = \frac{Y}{\ln 10\, I \sigma \tau}$$

I (einstein cm^{-2} s^{-1}): Irradiation intensity

σ (cm^2 mol^{-1}): Decadic extinction coefficient

τ (s): Time constant

Y: Chemical yield

Quantification of *N*-vanillylnonanamide (VN)

A solution of KFL-VN was irradiated in the same manner as other KFL-1 derivatives. After an appropriate irradiation period, a solution of 2Me4OMe-TokyoGreen (22) in DMSO was added as an internal standard for LC/MS analysis. Quantification of KFL-VN and VN was performed by LC/MS using a Waters ACQUITY UPLC H Class system equipped with an ACQUITY UPLC BEH C18 1.7 μm (2.1 × 50 mm) column. 10 mM formate ammonium buffer and acetonitrile were used as eluents. KFL-VN was quantified in terms of the absorption peak area in the chromatogram. VN ($[MH]^+$ (*m*/*z* = 294)) was monitored in the selective ion recording (SIR) mode and quantified in terms of MS peak intensity in the chromatogram. The peak area of KFL-VN and the MS peak intensity of VN were standardized based on the absorption peak area of 2Me4OMe-TokyoGreen. Standard solutions of VN (2, 5 and 10 μM DMSO) were used to prepare a calibration curve.

Strains

C. elegans strains were maintained under standard conditions (23). Wild-type worms were Bristol strain N2. Transgenic strains were obtained by standard microinjection techniques (24). *kyIs200* X[*sra6p::TRPV1*, *elt-2p::NLS-gfp*] was kindly provided by Cori Bargmann. All procedures were approved by Gene Recombination Experiment Safety Committee of Yamanashi University. The following transgenic strains were used:

ASH::GCaMP6s: *Ex*[*sra-6p::GCaMP6s 100 ng* μl^{-1}*, elt-2p::mRFP 20 ng* μl^{-1}]

ASH, PVQ::TRPV1 & GCaMP6s: *kyIs200* X; *Ex*[*sra-6p::GCaMP6s 100 ng* μl^{-1}*, elt-2p::mRFP 20 ng* μl^{-1}]

Body wall muscle::TRPV1 & GCaMP6s: *Ex*[*myo-3p::GCaMP6s 60 ng* μl^{-1}*, myo-3p::TRPV1::T2A-mCherry 60 ng* μl^{-1}]

HSN, GLR::GCaMP6s & TRPV1: *Ex*[*egl-6p::GCaMP6s 40 ng* μl^{-1}*, egl-6p::TRPV1::T2A-mCherry 100 ng* μl^{-1}*, myo-2p::mRFP 10 ng* μl^{-1}]

RIM::GCaMP6s & TRPV1: *Ex*[*tdc-1p::GCaMP6s 30 ng* μl^{-1}*, tdc-1p::TRPV1::T2A-mCherry 100 ng* μl^{-1}*, elt-2p::mRFP 30 ng* μl^{-1}]

AVA::GCaMP6s & TRPV1: *Ex*[*rig-3p::GCaMP6s 30 ng* μl^{-1}*, rig-3p::TRPV1::T2A-mCherry 100 ng* μl^{-1}*, elt-2p::mRFP 30 ng* μl^{-1}]

ASK::GCaMP6s: *Ex*[*sra-7p::GCaMP6s 60 ng* μl^{-1}*, elt-2::mRFP 30 ng* μl^{-1}]

ASK::GCaMP6s: *Ex*[*sra-9p::GCaMP6s 50 ng* μl^{-1}*, sra-9p::TRPV1::T2A-mCherry 100 ng* μl^{-1}*, elt-2p::mRFP 30 ng* μl^{-1}]

Molecular Biology

In this study, In-Fusion (Clontech) or Gibson Assembly (New England Biolabs) technology was used to obtain the constructs. Promoters such as *sra-6p* (4 kb), *elt-2p* (5.1 kb), *egl-6p* (3.8 kb), *tdc-1p* (4.4 kb), *rig-3p* (4.3 kb), *sra-7p* (4.1 kb), *sra-9p* (3kb), and *myo-2p* (1 kb) were amplified by PCR from wild-type genomic DNA and inserted into the L3558 plasmid (a gift from Andrew Fire (Addgene plasmid # 1550)) in which *gfp* was replaced by *GCaMP6s* or *mRFP*. GCaMP6s and mRFP were amplified by PCR from Prab-3::NLS::GCaMP6s (a gift from Andrew Leifer (Addgene plasmid # 68119)) (25) and pcDNA3-mRFP (a gift from Doug Golenbock (Addgene plasmid # 13032)) respectively. Rat *trpv-1* was amplified by PCR from genomic DNA of *kyIs200* X and inserted into L3558 plasmid in which *gfp* was replaced by *T2A-mCherry*. Primers used for PCR are listed in **Table S2**.

Uncaging of KFL-VN and calcium imaging

Escherichia coli (strain OP50) was scraped from the lawn on an LB agar plate or concentrated from the LB medium by centrifugation and mixed with KFL-VN (**5**) or KFL-1-mOPh-4-OMe (**2**) (control) stock solution in DMSO and M9 buffer to make a final concentration of 0.5 mM (for ASH and body wall muscles) or 1 mM (for HSN, RIM, AVA, PVQ, GLR, ASK). Boiling the bacteria (98°C for 30 min) before mixing with compounds may enhance the compound uptake by worms (26). The violet KFL-VN-OP50 mixture was spread onto Nematode Growth Medium (NGM) agar plates and allowed to dry for a few minutes. Young adult worms were cultivated on the bacteria-KFL-caged compound-seeded NGM plates in the dark for 0.5-4 h at room temperature. Fluorescence imaging was conducted using an Olympus IX73 inverted microscope with an ORCA-Flash4.0 V3 Digital CMOS camera C13440-20CU (Hamamatsu Photonics) and HCImageLive software (Hamamatsu Photonics). GCaMP6s was excited by strobed (10% duty cycle) 470 nm light (SOLIS-470C, ThorLabs). Caged compounds were excited by constant illumination at 580 ± 20 nm (2.4 mW mm^{-2}) from a 130 W mercury vapor lamp (U-HGLGPS, Olympus) equipped with a PB0580-020 filter (Asahi Spectra). The light stimulation for uncaging was controlled using an electronic shutter (SH1/M and SC10, ThorLabs). To constrain worm movement, worms were loaded into a custom-fabricated polydimethylsiloxane (PDMS) microfluidic device (olfactory chip) (27) using S basal buffer with 1 mM levamisole (Wako) (for optical control of body wall muscles, levamisole was removed). Fluorescence images were captured at 10 frame s^{-1}. For monitoring ASH activity, worms were pre-exposed to blue excitation light for 2-3 min in order to eliminate blue light-evoked Ca^{2+} transients (27).

To immobilize worms for confocal imaging (**Figure S4**), Pluronic F-127 hydrogel was used (28). Worms were picked up and transferred into an 8-well chamber slide with 200 µl of chilled hydrogel (4°C) containing 10% Pluronic F-127 (Sigma) and 1 mM levamisole (Wako). The chamber slide was

incubated at 13~15°C for 10 min to allow the worms to settle to the bottom. Uncaging and optical recordings of neural activity were performed using a TCS SP5 confocal microscope system (Leica). Fluorescence images were captured at 1 frame s^{-1} using a Leica Application Suite Advanced Fluorescence (LAS-AF) with a HCX PL APO CS 40.0×/1.25-0.75 objective lens (Leica). The excitation light source was a SuperK white-light laser coupled to an SP5 system. The excitation wavelengths for imaging were 495 nm for GCaMP6s and 575 nm for KFL-VN. Detection wavelengths were 510-540 nm for GCaMP6s and 585-630 nm for KFL-VN. Excitation light for uncaging was delivered at 565, 575, 585 nm (100% each).

Image processing and data analysis

Image processing was carried out using Fiji software (29) to generate images of the normalized fluorescence change of GCaMP6s ($\Delta F/F_0$). The resting fluorescence (F_0) image was generated by averaging the frames acquired before light irradiation. The fluorescence change from F_0 ($\Delta F = F\text{-}F_0$) was calculated by subtracting the F_0 image from all frames and divided by the F_0 image using the Image Calculator tool to obtain $\Delta F/F_0$ image stacks (**Figure S4B**). Noise reduction was done with a median filter plugin. For quantification of neural activity, custom MATLAB scripts were used. Briefly, the mean value of fluorescence intensity (F) of GCaMP6s was obtained by defining a circular region of interest (ROI) surrounding the cell body of each neuron. After subtracting local background fluorescence from the raw fluorescence, F_0 was calculated by averaging F values before irradiation (time = 0-5 s). The percent change in fluorescence intensity relative to F_0 was calculated ($\Delta F/F_0 = (F\text{-}F_0)/F_0 \times 100$ (%)) and plotted as a function of time. For statistical analysis of Ca^{2+} responses, peak $\Delta F/F_0$ was defined as the maximum value in the range from the start of light irradiation to the last frame. For AVA neurons, peak $\Delta F/F_0$ was defined as the maximum value during 20 s from the start of light irradiation (10-30 s), because AVA showed spontaneous oscillatory activity during Ca^{2+} imaging (**Figure 6F**). The onset latency for neuronal cells was defined as the time after light onset to the point where $\Delta F/F_0$ showed an increase of at least two standard deviations from the mean during five seconds before light onset.

The fluorescence intensity of body wall muscles and the worm body length in **Figure 5C** were measured using custom MATLAB scripts. Briefly, a rectangular ROI surrounding the whole body was manually defined for quantifying GCaMP fluorescence intensity. Based on GCaMP fluorescence in body wall muscles, the worm body was segmented automatically using standard MATLAB functions (e.g., edge, imdilate, imfill, bwpropfilt). The body length from the head to the tail (L) was measured using the bwferet function. In cases of failure to segment, the positions of the head and tail were determined manually. The baseline body length (L_0) was calculated by averaging L values during the first five seconds. The relative body length was defined as L/L_0.

Behavioral assays

KFL-VN was mixed with H_2O and *E. coli* to give a concentration of 535 μM for ASH and 1 mM for RIM and AVA. The mixture was spread on NGM agar plates and dried for a few minutes. Young adult worms were incubated on the bacteria-KFL-caged compound-seeded NGM plates in the dark for at least 30 minutes for ASH and 3 h for RIM and AVA at room temperature. All the behavioral assays were carried out on unseeded NGM agar plates using a fluorescence stereomicroscope SZX7 (Olympus) equipped with a 130 W mercury vapor lamp (U-HGLGPS, Olympus). Each worm's behavior was recorded at 10 frames s^{-1} using an ORCA-Flash4.0 V3 Digital CMOS camera C13440-20CU (Hamamatsu Photonics) and HCImageLive software (Hamamatsu Photonics). The whole-body illumination was conducted at 545-580 nm (2.5 mW mm^{-2}) for about 5 s using a mirror unit SZX2-MRFP (Ex 545-580/Em 610-, Olympus). Worms initiating backward movement during the 5 s irradiation were scored as 1. Worms showing forward movement or backward movement after the end of irradiation were scored as 0. The fraction of worms responding to light irradiation was calculated.

Statistical analysis

Statistical analyses was done with R software (30). The statistical method used for comparison is stated in the figure legends, together with the sample size (*n*) and the statistical significance compared with the controls (*$P < 0.05$, **$P < 0.01$, ***$P < 0.001$).

Microfluidic device fabrication

The microfluidic behavioral arena was prepared using standard soft lithography(31). The photomask of the arena was designed in CAD software (AutoCAD, Autodesk) according to a previous report (1). The silicon mold master was created by patterning a 78 μm layer of SU-8 3050 photoresist (Nippon Kayaku Co., Ltd., Japan) on a Si wafer. Then, polydimethylsiloxane (PDMS) was prepared by mixing a silicone elastomer and curing agent (Silpot 184, Dow Corning Toray) at a 10:1 ratio, degassed, and cast in the mold to form a 5-mm-thick device. The PDMS was baked at 65 °C for 1.5 h, and then inlet and outlet holes were cored with a 19G syringe needle. The PDMS device was cleaned in 100% ethanol overnight and baked at 65 °C for 1 h to evaporate any absorbed ethanol.

Experimental setup of the microfluidic device

The general experimental setup was as described in the literature (32). Briefly, the microfluidic arena was assembled by sealing the PDMS casting between 50 × 50 × 3 mm glass plates and clamped with binder clips. The upper glass plate was drilled with a diamond-coated bit for tubing connections. The device was degassed in a vacuum for 5-10 min before loading a 5% (w/v) Pluronic F127 solution through the outlet port and flushed with S-basal buffer (100 mM NaCl, 50 mM potassium phosphate

buffer pH 6.0) by connecting tubing from the 20-ml syringe reservoirs to the arena. About 26 worms were gently injected via a syringe into the arena. The microfluidic device containing the worms was placed on a glass monitor stand and illuminated from below with LED light. A video of the animals' behavior was taken at ~45 pixels mm^{-1} and 2 frames s^{-1} using a USB3 Vision camera DN3V-200BU (Shodensha) and a zoom lens L-870 (Hozan). During video capture, buffer flow from the reservoir was driven by gravity. After each experiment, the PDMS devices were washed with water, soaked in 100% ethanol overnight, and baked at 65 °C for 1 h. The devices were reused after this cleaning procedure.

Data analysis of behavioral experiments in a microfluidic device

The videos of worms were analyzed using MATLAB-based worm-tracking software (1). In **Figure S5D**, speed and behavioral state probabilities were averaged across 5-s bins and all experiments. Since the videos were captured at 2 frames s^{-1}, a 5-s bin contains 10 frames. Thus, the sample size is calculated as follows: n = 6 experiments × 10 frames = 60 frames per time bin for *kyIs200* X and n = 5 experiments × 10 frames = 50 frames per time bin for wild type.

Supplementary References

1. Albrecht DR & Bargmann CI (2011) High-content behavioral analysis of *Caenorhabditis elegans* in precise spatiotemporal chemical environments. *Nat. Methods* 8(7):599-605.
2. Chen TW*, et al.* (2013) Ultrasensitive fluorescent proteins for imaging neuronal activity. *Nature* 499(7458):295-300.
3. Lin JY, Knutsen PM, Muller A, Kleinfeld D, & Tsien RY (2013) ReaChR: a red-shifted variant of channelrhodopsin enables deep transcranial optogenetic excitation. *Nat. Neurosci.* 16(10):1499-1508.
4. Umeda N*, et al.* (2014) Boron dipyrromethene as a fluorescent caging group for single-photon uncaging with long-wavelength visible light. *ACS Chem. Biol.* 9(10):2242-2246.
5. Inoue M*, et al.* (2019) Rational engineering of XCaMPs, a multicolor GECI suite for in vivo imaging of complex brain circuit dynamics. *Cell* 177(5):1346-1360.e1324.
6. Larsch J*, et al.* (2015) A circuit for gradient climbing in *C. elegans* chemotaxis. *Cell Rep.* 12(11):1748-1760.
7. Akerboom J*, et al.* (2013) Genetically encoded calcium indicators for multi-color neural activity imaging and combination with optogenetics. *Front. Mol. Neurosci.* 6(2).
8. Umezawa K, Nakamura Y, Makino H, Citterio D, & Suzuki K (2008) Bright, color-tunable fluorescent dyes in the visible-near-infrared region. *J. Am. Chem. Soc.* 130(5):1550-1551.
9. Troemel ER, Chou JH, Dwyer ND, Colbert HA, & Bargmann CI (1995) Divergent seven transmembrane receptors are candidate chemosensory receptors in *C. elegans*. *Cell*

83(2):207-218.

10. Zheng Y, Brockie PJ, Mellem JE, Madsen DM, & Maricq AV (1999) Neuronal control of locomotion in *C. elegans* is modified by a dominant mutation in the GLR-1 ionotropic glutamate receptor. *Neuron* 24(2):347-361.
11. Tobin D*, et al.* (2002) Combinatorial expression of TRPV channel proteins defines their sensory functions and subcellular localization in *C. elegans* neurons. *Neuron* 35(2):307-318.
12. Guo M*, et al.* (2015) Reciprocal inhibition between sensory ASH and ASI neurons modulates nociception and avoidance in *Caenorhabditis elegans*. *Nat. Commun.* 6:5655.
13. Schmitt C, Schultheis C, Husson SJ, Liewald JF, & Gottschalk A (2012) Specific expression of channelrhodopsin-2 in single neurons of *Caenorhabditis elegans*. *PloS one* 7(8):e43164.
14. Alkema MJ, Hunter-Ensor M, Ringstad N, & Horvitz HR (2005) Tyramine functions independently of octopamine in the *Caenorhabditis elegans* nervous system. *Neuron* 46(2):247-260.
15. Schwarz V, Pan J, Voltmer-Irsch S, & Hutter H (2009) IgCAMs redundantly control axon navigation in *Caenorhabditis elegans*. *Neural Development* 4(1):13.
16. Macosko EZ*, et al.* (2009) A hub-and-spoke circuit drives pheromone attraction and social behaviour in *C. elegans*. *Nature* 458(7242):1171-1175.
17. Davis MW, Morton JJ, Carroll D, & Jorgensen EM (2008) Gene activation using FLP recombinase in *C. elegans*. *PLoS Genet.* 4(3):e1000028.
18. Gordus A, Pokala N, Levy S, Flavell Steven W, & Bargmann Cornelia I (2015) Feedback from network states generates variability in a probabilistic olfactory circuit. *Cell* 161(2):215-227.
19. Dobosiewicz M, Liu Q, & Bargmann CI (2019) Reliability of an interneuron response depends on an integrated sensory state. *eLife* 8:e50566.
20. Mao T, O'Connor DH, Scheuss V, Nakai J, & Svoboda K (2008) Characterization and subcellular targeting of GCaMP-type genetically-encoded calcium indicators. *PloS one* 3(3):e1796.
21. Tian L*, et al.* (2009) Imaging neural activity in worms, flies and mice with improved GCaMP calcium indicators. *Nature Methods* 6(12):875-881.
22. Urano Y*, et al.* (2005) Evolution of fluorescein as a platform for finely tunable fluorescence probes. *J. Am. Chem. Soc.* 127(13):4888-4894.
23. Brenner S (1974) The genetics of *Caenorhabditis elegans*. *Genetics* 77(1):71-94.
24. Mello CC, Kramer JM, Stinchcomb D, & Ambros V (1991) Efficient gene transfer in *C.elegans*: extrachromosomal maintenance and integration of transforming sequences. *EMBO J.* 10(12):3959-3970.
25. Nguyen JP*, et al.* (2016) Whole-brain calcium imaging with cellular resolution in freely behaving *Caenorhabditis elegans*. *Proc. Natl Acad. Sci.* 113(8):E1074-E1081.
26. Zheng S-Q, Ding A-J, Li G-P, Wu G-S, & Luo H-R (2013) Drug absorption efficiency in

Caenorhbditis elegans delivered by different methods. *PloS one* 8(2):e56877.

27. Chronis N, Zimmer M, & Bargmann CI (2007) Microfluidics for in vivo imaging of neuronal and behavioral activity in Caenorhabditis elegans. *Nature Methods* 4:727.

28. Hwang H, Krajniak J, Matsunaga Y, Benian GM, & Lu H (2014) On-demand optical immobilization of *Caenorhabditis elegans* for high-resolution imaging and microinjection. *Lab Chip* 14(18):3498-3501.

29. Schindelin J*, et al.* (2012) Fiji: an open-source platform for biological-image analysis. *Nat. Methods* 9(7):676-682.

30. Team RC (2012) R: A language and environment for statistical computing (R Foundation for Statistical Computing, Vienna, Austria).

31. Duffy DC, McDonald JC, Schueller OJA, & Whitesides GM (1998) Rapid prototyping of microfluidic systems in poly(dimethylsiloxane). *Analytical Chemistry* 70(23):4974-4984.

32. Lagoy RC & Albrecht DR (2015) Microfluidic devices for behavioral analysis, microscopy, and neuronal imaging in *Caenorhabditis elegans*. *C. elegans: Methods and Applications*, eds Biron D & Haspel G (Humana Press, Totowa, NJ), pp 159-179.